Superconducting Artificial Atoms

BSc Project PH3110 Report

Kristiyan Dilov

Supervisor: Prof. Oleg Astafiev

March 12, 2021

Abstract

Quantum computers are more powerful than classical computers because they are based on the fundamental principles of quantum mechanics, like superposition, quantum tunneling and entanglement. In this project, we will go through all the important theoretical and experimental concepts which shape the quantum computer. The fabrication process of qubits, the heart of quantum computers, will be explored. Furthermore, data of various phenomena will be gathered and analysed using Python.

1 Introduction

A qubit is a quantum mechanical analogue of a classical bit. With today's technology, it is possible to fabricate particles of metal a few hundred angstroms in size. Electrons in these structures are regarded as artificial atoms - atoms whose effective nuclear charge is controlled by metallic electrodes. These small electronic systems contain discrete number of electrons and a discrete spectrum of energy levels. Artificial atoms are used as quantum bits (qubits). A qubit is the basic unit of quantum information. For example, they can be realised as an electric circuit made of superconducting components. Theoretically, a qubit is a two-level system. A two-level system is a quantum system that can exist in a superposition of two energy states $|0\rangle$ and $|1\rangle$. Any two-level system can be seen as a qubit. In comparison to a classical computer, where we have binary digits 0 and 1 as means of storing information, in a qubit, there is $|0\rangle$ and $|1\rangle$ states encoding the bits and a coherent superposition of both. There are three types of qubits: flux qubit, phase qubit and charge qubit [1]. To create a solid-state qubit, a two-level quantum system must be isolated from the environment and cooled in order to avoid errors in qubit operations that could overwhelm the system [2].

There are three key factors which prevent the quantisation of a circuit. First, there are a lot of electrons going through it so their discrete nature disappears. Second, temperature is related to energy stored in the random movement of atoms, hence, classical randomness related to temperature is different from quantum randomness. Thirdly, there is energy loss due to electrical resistivity which in turn hides quantum effects. What circuits and atoms have in common is that they both are influenced by the laws of electrodynamics and quantum mechanics. Superconductivity is the discovery which pushes circuits in the quantum regime since electrons bond together to form Cooper pairs.

Since electrons have spin 1/2, they are fermions. When combined, they form a Cooper pair with total spin 0 or 1, hence it is a composite boson and its wavefunction is symmetric under particle exchange. Cooper pairs do not lose energy while transferring charge. Superconductors have this advantage because they can stimulate the formation of Cooper pairs. A Cooper pair is formed via electron-phonon interaction. An electron in the cation lattice will distort the lattice around it, creating an area of greater positive charge density around itself. Another electron at some distance in the lattice is then attracted to this charge distortion (phonon). Thus, the electrons are indirectly attracted to each other and form a Cooper-pair. However, if the temperature exceeds the energy of the Cooper pair bond (the superconducting gap) the electrons will then be broken up and resistance will again become present. This is the reason superconductivity has a threshold temperature [3].

Superconductors have no electrical resistance. If metals are cooled to extremely low temperatures (-273°C = 0 K, absolute zero) some of them become superconductors. After fabrication of the qubit, the process of measurement follows. It is placed in cryogenic conditions in order to function as a superconductor and microwaves are sent to the chip. The qubit is also connected to a resonator, in order to increase time range of coherence.

In the first part of the report, the theoretical basis will be explained. Next, the fabrication process of the qubits will be described. The third part will consider the experimental setup, measurements and experiments performed on the qubit. Finally, data analysis will be explored for phenomena such as resonant frequency, relaxation time data T_1, Rabi oscillations and effect of magnetic field on angular frequency.

2 Theory

2.1 Quantum Harmonic Oscillator

Quantum Harmonic Oscillator is analogous to classical oscillator. It models the molecular vibrations of systems. We will find the allowed Energies E in the time independent Schrodinger equation

$$-\frac{\hbar^2}{2m}\frac{\mathrm{d}^2\psi}{\mathrm{d}x^2}+\frac{1}{2}m\omega^2x^2\psi(x)=E\psi(x). \tag{1}$$

It is required the wavefunction $\psi(x)$ to be symmetric about x=0 so that it is normalizable. After using power series and boundary conditions we get

$$E_n=\left(n+\frac{1}{2}\right)\hbar\omega=\frac{2n+1}{2}\hbar\omega, \tag{2}$$

where n is an integer. Several important features appear. First, the energy is quantized with allowed values only in equation (2). In addition, the allowed energies are evenly spaced

$$E=E_{n+1}-E_n=\hbar\omega=hf. \tag{3}$$

A particle in high energy state will emit a photon with energy equal to hf and will lower its energy state. A particle will make a transition from lower energy state to higher after absorbing a photon with the same energy [4]. In theory, the Quantum Harmonic Oscillator has infinite energy levels. However, if we consider only two energy levels (eigenstates), ground and excited, we get a two-level system. A two-level system is a quantum system which exists in superposition of two independent states

$$|\psi\rangle = c_1|1\rangle + c_2|2\rangle. \tag{4}$$

Where $|1\rangle$ and $|2\rangle$ are the states of the system and c_1 and c_2 are probability amplitudes.

2.2 Quantum decoherence and Superconductivity

Particles are described using wavefunctions. When two particles have a phase relation, it is said they are coherent (in superposition). This is needed for quantum computers to function since superposition offers the exponential increase in memory storage. Superposition helps go away from binary constraints. Hence, qubits are used for quantum computing because they can have superposition of $|0\rangle$ and $|1\rangle$. This is how quantum information is encoded on quantum states.

When a measurement is performed, coherence is shared with the environment and it is lost, hence called decoherence. Decoherence is the disappearance of superposition of quantum states. It is a mechanism that recovers classical behaviours from a quantum system. In addition, dephasing time (or spin-spin relaxation) is the time it takes the system to lose its quantum behaviour [5]. The evolution of a quantum system is described by the Shrödinger equation,

$$i\hbar\frac{\partial}{\partial t}|\psi\rangle = \hat{H}|\psi\rangle, \tag{5}$$

which is true for a system in isolation. There is also evolution when performing a measurement, which is the infamous collapse,

$$|\psi\rangle = \sum_n c_n|n\rangle \rightarrow |n_i\rangle. \tag{6}$$

Equation 6 is called the "first intervention" and it represents the wave collapse. The superposition of states collapses on one eigenstate, the measurement.

Another factor which influences the performance of a quantum computer is quantum noise. Quantum noise is noise which arises from quantum fluctuations. It represents the uncertainty of both amplitude and phase. Quantum noise refers to the fluctuations of signal in extremely precise systems. It is reasonable to consider quanta appearing or disappearing spontaneously in spacetime due to the most basic laws of conservation. Thus, quantum error correction is essential in protecting quantum information. Altough it is not possible to copy quantum information, a popular method is using quantum error correcting code by storing information of one qubit onto a highly entangled state of nine qubits [6].

Below a certain temperature, there is a range of materials (for example, Aluminium) that conduct electricity without resistance. This phenomenon is superconductivity. If there is a weak external magnetic field, it will not penetrate the material but remain at its surface. Electrons form Cooper-pairs which move inside the solid without friction. The solid is considered a lattice of positive ions in a cloud of electrons. Due to the attractive forces between the two mediums, their movements generate electricity. The bond in a Cooper pair is very weak and the pair can be broken up by thermal energy. Thus, superconductivity occurs only at low temperature. There are two types of superconductors, Type I remain superconducting only with weak magnetic fields while Type II can be superconducting with strong magnetic fields [26].

2.3 Bloch sphere

The Bloch sphere is a graphical representation of quantum states of a two-level system as shown on Figure 1. The north pole is the ground state $|0\rangle$ while the south pole is the excited state $|1\rangle$. The poles present classical bits, everything else around the surface of the sphere represents quantum bits. When a qubit is measured or it interferes with the environment, it collapses on one of the two poles. Thus, it is important to isolate the qubit from outside influences [9].

A quantum state is a mathematical concept that provides a probability distribution for the outcomes of each possible measurement on a system. Quantum states that cannot be written as a mixture of other states are called pure quantum states and all the other states are called mixed quantum states. Any pure quantum state $|\psi\rangle$ in a two-level quantum system can be written as a superposition of $|0\rangle$ and $|1\rangle$,

$$|\psi\rangle = \cos\frac{\theta}{2}|0\rangle + e^{j\phi}\sin\frac{\theta}{2}|1\rangle. \tag{7}$$

Where θ is the latitude angle in the range $\in [0, \pi)$ and ϕ is the longitude angle in the range $\in [0,2\pi)$.

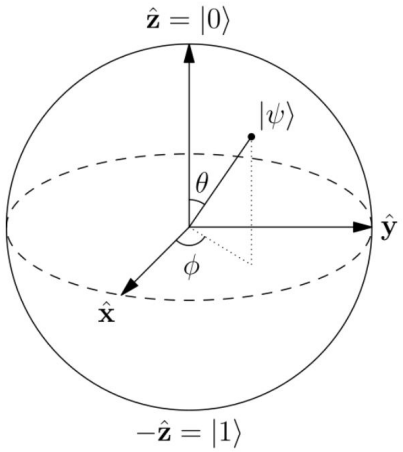

Figure 1: Bloch sphere. The points on the surface of the sphere correspond to pure states. The interior points correspond to mixed states [9].

2.4 Josephson effect

A essential circuit element is the Josephson Junction. A Josephson Junction is made of two superconducting layers (usually made of Al), separated by a thin insulating layer, which can experience tunnelling of Cooper pairs. The Cooper pairs can be represented as wavefunction which tunnel through the insulating layer, Figure 2. The Josephson devices make it easy to couple multiple qubits together. The AC Josephson effect is present when the voltage across the junction is proportional to the characteristic frequency. Then, the junction will oscillate with that characteristic frequency. The DC Josephson effect is present when a current is proportional to the phase difference of the wavefunctions, hence, the current can flow in the circuit in the absence of voltage, Equation 8 [10],

$$I(t) = I_c \sin(\varphi(t)), \tag{8}$$

where $\varphi(t)$ is the superconducting phase and I_c is the critical current. The critical current is the maximum current a material can carry with zero resistance. A current greater than I_c will cause the material to revert back to normal state. Below that current we have superconducting state. Josephson energy is defined as

$$E_J = \frac{\Phi_0 I_c}{2\pi}, \tag{9}$$

where $\Phi_0 = h/2e$ is the magnetic flux quantum and h is Planck constant. In addition, the energy stored in a Josephson junction can be represented as

$$E(\varphi) = E_J(1 - \cos(\varphi)). \tag{10}$$

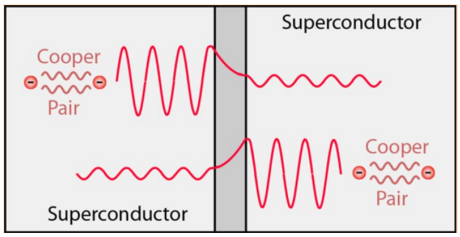

(a) All the Cooper pairs in a superconductor can be described with a single wavefunction since all pairs have the same phase ("phase coherent") [10].

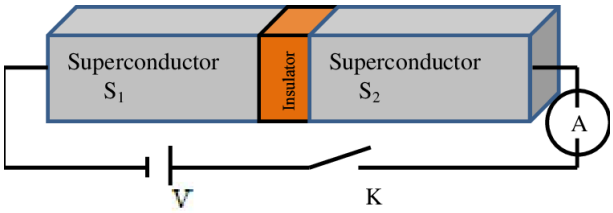

(b) Schematic diagram of AC Josephson junction [12].

Figure 2

2.5 Cooper-pair box

A Cooper-pair box (charged qubit) is a superconducting qubit with charged states as basis states, two charge states can be coherently superposed. It is a circuit which consists of gate voltage, capacitor and Josephson junction, Figure 3. The Cooper-pair box is based on the quantum harmonic oscillator but with anharmonicity present in the system. The charging Coulomb energy of the island of the box is defined as,

$$E_C = (2e)^2/2(C_g + C_J), \tag{11}$$

where e is the electric charge, C_g is the gate capacitor and C_J is the junction capacitance. Gate capacitance is the absolute capacitance of the gate of the circuit while Junction capacitance is the capacitance which forms in a PN junction diode under reverse bias.

By applying a gate voltage pulse we can control the coherent state evolution. Gate voltage controls the chemical potential of the island. A single Copper-pair box is useful because at very low temperatures, electrons form Cooper pairs and condense into a single ground state $|n\rangle$, where n is the charge number state with n number of electrons. We can also consider the Cooper-pair box as a two level system. Hence, the relative energy of the two levels can be controlled using the gate voltage. Circuits derived from the Cooper-pair box are called "charge qubits". The reason for that is because charge in "charge qubit" refers to the cotrolled variable, i.e. the qubit variable that couples to the control line we use to write or manipulate quantum information. Typical T_2 coherence times for a charge qubit go up to 1-2 μs. However, a type of charge qubit called transmon can last up to 100μs [8].

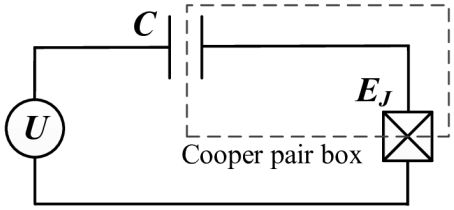

Figure 3: The dashed rectangle (island) contains Copper pairs which forms the qubit [7].

2.6 Transmon qubit

The transmon is a more developed type of charge qubit. It is insensitive to low-frequency charge noise at all operating points. The transmon qubit is very similar to the Cooper-pair box, except that an extra capacitor is placed between the gate and the island, see Figure 5. This lowers the charging energy $E_C = e^2/2C$ so the ratio E_J/E_C increases. This leads to steeper charge dispersion, meaning, energies change rapidly with the offset charge n_g. This means that the n_g dependence of energy levels can be eliminated, while preserving anharmonicity for qubit control. Anharmonicity is the deviation of a system from a harmonic two-level one. The transmon has decreased sensitivity to charge noise. The eigenenergies of the four lowest qubit levels can be seen on Figure 4. Figure 6 shows an image of an integrated transmon qubit. The Hamiltonian of the transmon is shown on equation 12, with $n = Q/2e$ called the charge variable [13].

$$\hat{H} = 4E_C(\hat{n} - n_g)^2 - \frac{E_J}{2}\sum_n |n+1\rangle\langle n| + |n+1\rangle\langle n|. \tag{12}$$

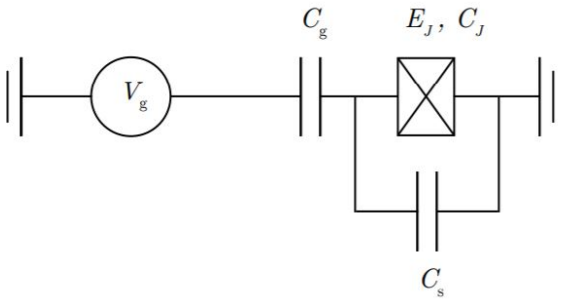

(a) Transmon qubit circuit [13].

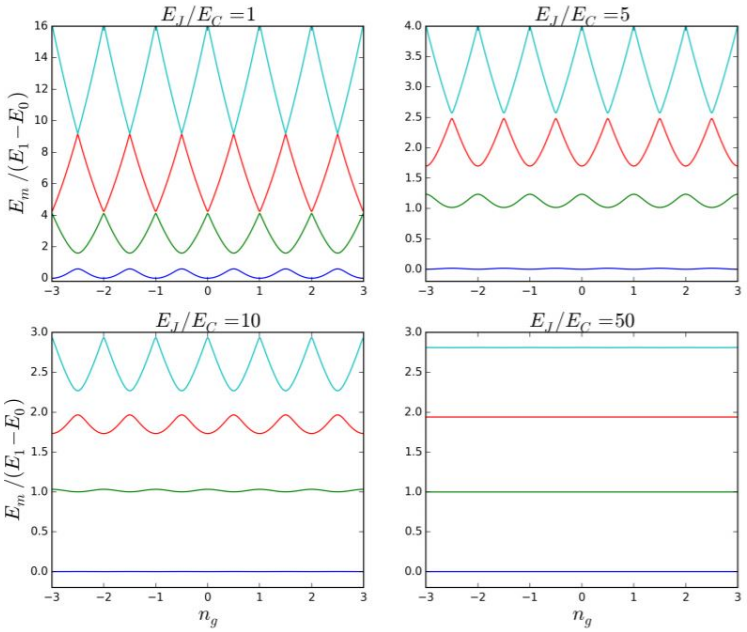

(b) The eigenvalues come from equation 13. First four energy levels as a function of n_g [13].

Figure 4

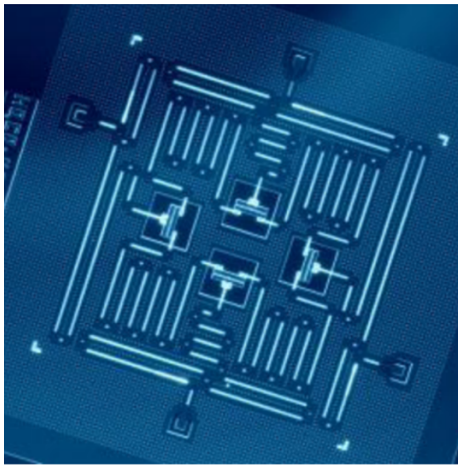

Figure 5: An example of a quantum processor with 4 transmon qubits and 4 resonators designed by IBM [14].

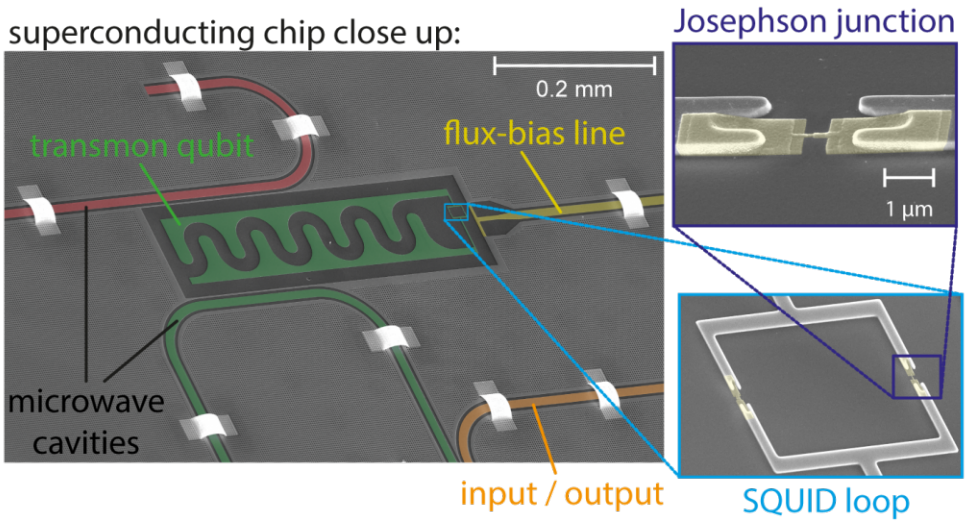

Figure 6: An integrated transmon capacitor. The cavity has length of several centimeters. A SQUID (superconducting quantum interference device) loop connects two Josephson Junctions. The green cavity is used to read the state of the transmon qubit. It is coupled to the orange cavity which registers the readout results [11]

2.7 Phase qubit

Compared to other qubits, phase qubits are physically larger from 1μm to 100μm. They also have the advantage of scalability, meaning, complex circuits can be constructed using microfabrication technology. Phase qubits have the largest capacitance and a characteristic resonator impedance close to 50Ω. This means that phase qubits can be more strongly coupled to transmission lines and resonator circuits. Phase qubits can also be wired over long distances. Impedance, however, will become a crucial parameter as the circuits become more complex. The Hamiltonian of the system is described with equation 13, where the last term describes the effect of the external bias current I_b (washboard potential) [15]. A diagram of phase qubit is shown in Figure 7

$$H = -E_C \partial_\phi^2 - E_J \left(\cos\phi + \frac{I_b}{I_c}\phi \right) \tag{13}$$

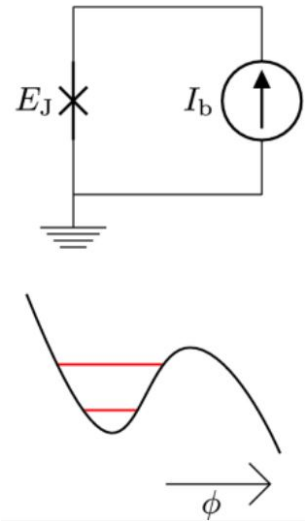

Figure 7: Diagram of phase qubit and its potential energy landscape. The two lowest energy levels are marked in red. ϕ is the phase difference as the coordinate of the washboard potential [47].

2.8 Flux qubit

Another way to realize the limit $E_J >> E_C$ is by using degeneracy between two current-carrying states of an RF-SQUID. The Hamiltonian now has to take into account the magnetic energy, hence

$$H = -E_C \partial_\phi^2 - E_J \cos\phi + E_L(\phi - \phi_x)^2/2 \tag{14}$$

where $\phi_x = 2\pi\Phi_x/\Phi_0$ is the reduced flux through the loop, and the inductive energy scale is given by $E_L = \Phi_0^2/4\pi L$. The coherence time of the flux qubit is significantly enhanced since no external degrees of freedom can interfere with the qubit due to the magnetic field. Flux qubits have weak sensitivity to charge noise comparatively easy readout and the ability to work at or near the degeneracy point. All operations on the qubit must be DS pulses only. Their main disadvantage is a very strong dependence on the junction parameters [16]. A diagram of flux qubit is shown in Figure 8

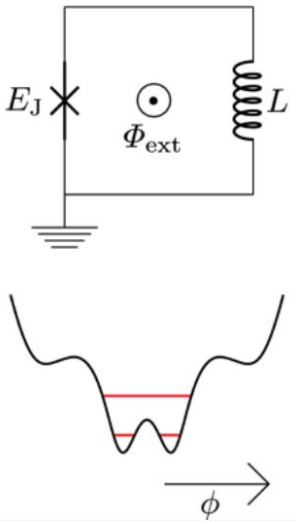

Figure 8: Diagram of flux qubit and its potential energy landscape. The two lowest energy levels are marked in red. ϕ is the phase difference across the Josephson junction as the coordinate [47].

3 Fabrication of Qubit

3.1 Silicon substrate with resist

Superconducting qubits are made on silicon (Figure 9) or sapphire wafers using electron beam lithography (EBL) and metallic thin film evaporation processes [8]. The wafer is covered with polymer liquid called resist.

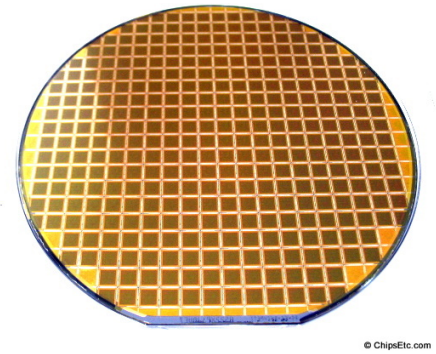

Figure 9: Silicon Wafer developed by Intel Corp. Silicon is a semiconducting material and it is the building block of qubits [18].

The resist is used as a mask to cover areas of the wafer which should not be doped (only in photolithography processes). There are two types of resit, positive and negative. The positive resist has solubly exposed areas, has excellent resolution and is stable against developers. The negative resist has insolubly exposed areas, good adhesion on the wafer but has lower resolution [19]. It is then placed inside a centrifuge to cover it uniformly, see Figure 10. Depending on the process, at 2000 to 6000 rpm the resist layer can be up to 2 microns. The thickness depends on how fast the chuck rotates and the viscosity of the resist [19].

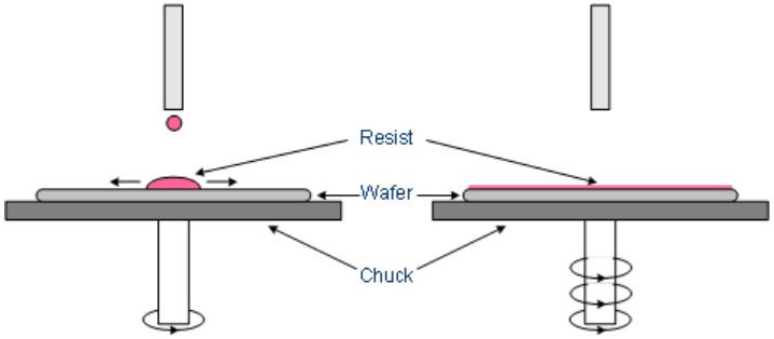

Figure 10: The coating of the wafer is done via a rotating chuck [19].

3.2 Photolithography

Photolithography is the method of using light to make the conductive paths on silicon wafers of microprocessors using a Photolitographer (Figure 11a) [20]. It is used only when the layer of resist is micrometers in size or we have a large structure. The coated structure is then exposed to UV light radiation, Figure 11b. Photolithography mask is an opaque plate or film with transparent areas that allow light to shine through in a defined pattern. It is commonly used to cover certain areas which should not be doped. It is important to note that if the wafer is overexposed to the UV light, the resist patterns will be small with big holes. If it is underexposed, the resist patterns will be large with small holes. Another factor is bad focusing which leads to unexposed areas [19].

In the end, a solvent called developer is applied. If the resist was positive, the developer dissolves only the regions that were exposed to light. If the resist was negative, the developer will dissolve only the regions that were not exposed to light, leaving the coating on light-exposed regions.

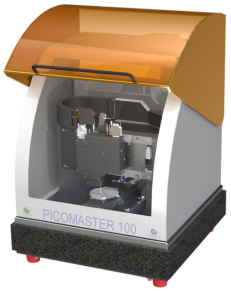

(a) Example of Photolitographer [21].

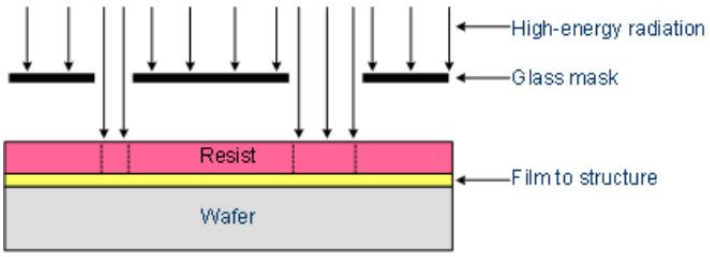

(b) Glass mask is used so that the areas of interest are exposed only [19].

Figure 11

3.3 Electron Beam Lithography (EBL)

In the case of a very thin resist layer or when using small structures, we apply Electron Beam Lithography. This is very similar to Photolithography but here an electron beam is used. However, with EBL we can produce complex features on the substrate with very high resolution and precision, see Figure 12. Here, patterns are directly engineered on the substrate without the need of a mask. Another advantage of EBL is that it is not diffraction-limited unlike photolithography. Resolutions up to 10 nm can be produced. On the other hand, it takes a longer time to apply it [22].

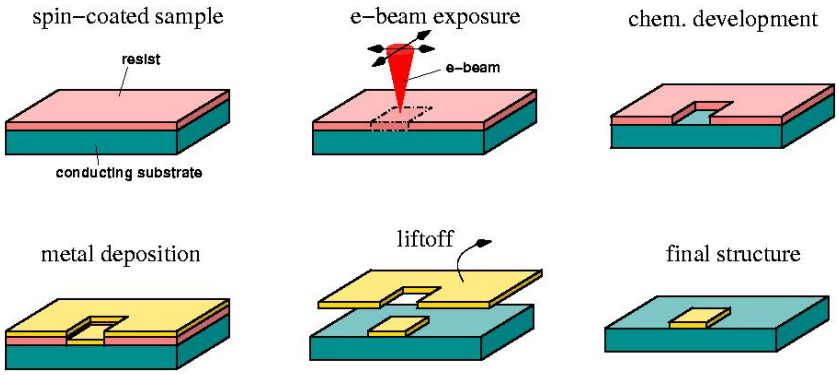

Figure 12: Diagram of EBL process using electron beams to draw the canals. The EBL process is in vacuum [22].

3.4 Deposition

The next step of the fabrication process uses Plassys electron beam evaporator, see Figure 13a. The device uses a vapor deposition tool that uses an intense electron beam to vaporize a source metal which is placed in a chamber under high vacuum. In manufacturing qubits, superconductor (like aluminium) is used as a source metal to be melted. Thus, molecules and atoms evaporate freely in the chamber and they condense on the surface of the substrate, creating the superconducting circuit on the chip [23]. There are two types of deposition, chemical vapour deposition (CVD) and physical vapour deposition (PVD). In this experiment, PVD is applied with temperatures in the range of 200 - 400°C. This produces thin-film coating in the range 1 to 10 micrometers [24]. A diagram of the process can be seen on Figure 13b. Finally, a chemical called Remover is used to remove the resist with metal film from the substrate.

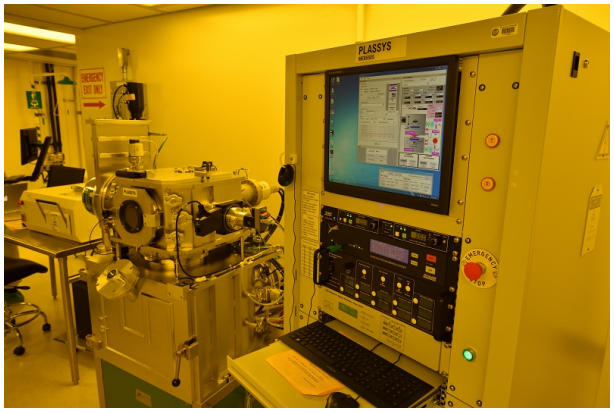

(a) Plassys Electron Beam Evaporation System [23].

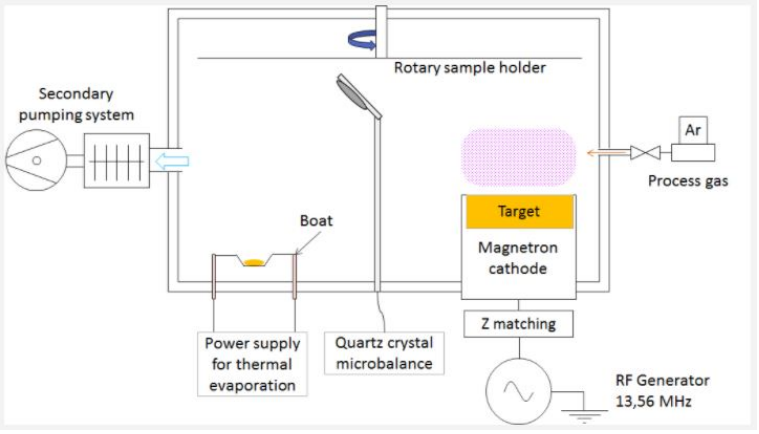

(b) Diagram of the Plassys [25].

Figure 13

4 Measurement

4.1 Experimental setup

Figure 14a shows the whole experimental setup. Arrow 1 points at the Vector Network Analyzer. It is used to send and receive microwaves to and from the system and record measurements. Arrow 2 shows the device used to change the magnetic field B. Arrows 3 and 4 point at the signal and phase generator respectively. They are used to send specific signals to the qubit. Everything is connected to the cryostat, arrow 5. Inside are the cables going from top to bottom. The whole system is a dilution refrigerator and is kept under cryogenic conditions.

Figure 14b shows a diagram inside the Dilution Refrigerator refrigerator. We can see from the figure, the VNA sends signals which go through the disks. Thanks to the attenuators (red boxes on input line), they suppress black body radiation without distorting the waveform. Inside the chip, the transmon qubit is attached to a resonator via a coupling capacitor C_c. The transmon is also attached to a SQUID which detects the changes in magnetic field. The SQUID (superconducting quantum interference device) is a sensitive magnetometer. A computer is used to change the current which changes the magnetic field at the Coil and manipulates the Josephson energy E_J in the SQUID, thus influencing the qubit. Next, the qubit returns the signal upwards via the output cable. The isolators on the diagram allow the signal to go upwards without dissipation even with increasing temperature, hence reaching the VNA.

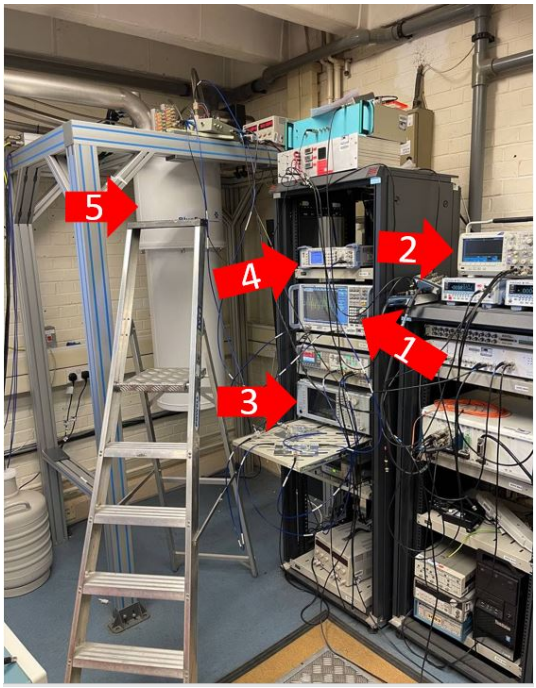

(a) Experimental setup.

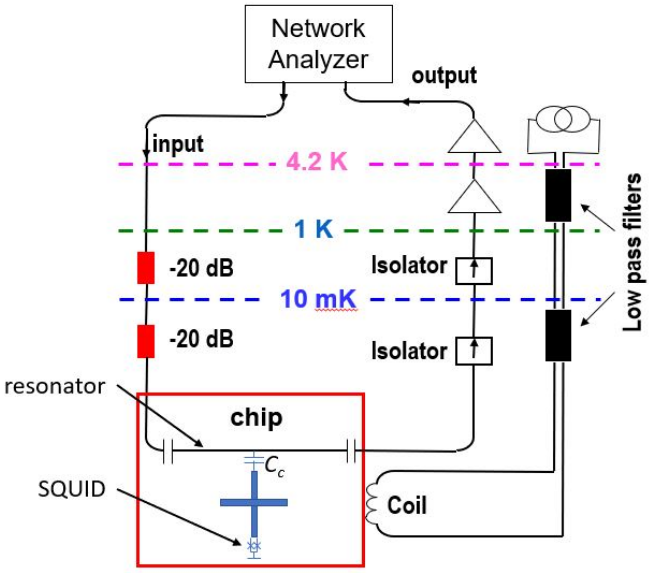

(b) Diagram of the process inside Dilution Refrigerator. The blue cross inside the red chip box is a transmon qubit with a SQUID attached at the bottom.

Figure 14

4.2 Dilution Refrigerator

The qubit is placed in a dilution refrigerator to keep it in cryogenic conditions (10mK). In order to increase the coherence time, we couple the qubit to a resonator. We perform frequency manipulations on the qubit using a vector network analyser (VNA). Then, a signal is sent back to the VNA where it is interpreted. The objective of the experiment at this stage is to measure the resonant frequencies and gather the parameters of the transmon qubit. There are three discs each with lower temperatures. The final disk reaches 10mK.

The Dilution Refrigerator is a device used to reach cryogenic temperatures below 1K, see Figure 15. A mixing chamber is created containing separated 3He and 4He below 0.8K. At 1K, vapour pressure of 3He is higher than 4He, then the 4He rich zone can be pumped removing 3He atoms. Energy is needed to move a 3He atom into the 4He zone. The 3He leaves the mixing chamber in the dilute phase. On the dilute side and in the still the 3He flows through superfluid 4He which is at rest. Hence, this causes the mixture to cool [27].

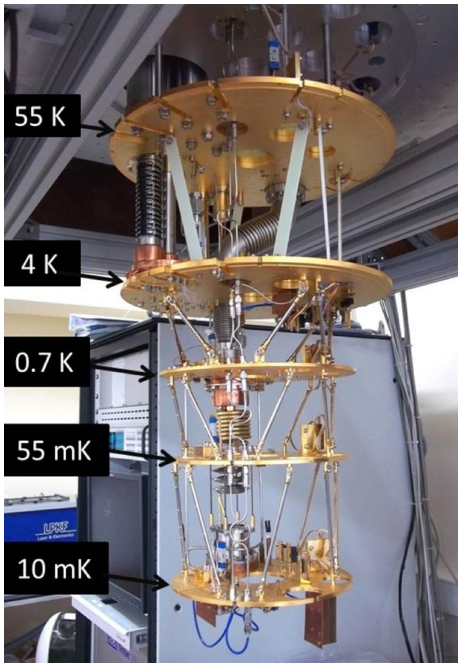

Figure 15: Dilution refrigerator. It uses the mixture of 3He and 4He isotopes to cool below 1K [29].

4.3 Rabi oscillations

A two-level quantum system coupled to a electromagnetic resonator in the presence of oscillatory driving field has a cyclic behaviour called Rabi cycle. The inverse of the Rabi cycle is the Rabi frequency, equation 15. If the system is illuminated with a beam of photons, it will cyclically absorb and emit them via stimulated emission

$$\Omega = \sqrt{(\omega - \omega_0)^2 + \omega_1^2}. \tag{15}$$

Where ω is the applied frequency, $\omega_0 = \gamma B_0$ and $\omega_1 = \gamma B_1$ with $\gamma = e/m_e c$ being the gyromagnetic ratio. At $\omega = \omega_0$ we have resonance [31].

Quantum oscillations can be observed in a Cooper-pair box using a charge degree of freedom. Coherent control of the qubit state can be achieved by applying resonant microwave excitations. When the applied microwave frequency equals the energy difference of the qubit, the qubit oscillates between the ground state and the excited state (Rabi oscillations). The Rabi frequency depends linearly on the microwave frequency. At certain set of applied frequencies, there will be observed absorption peaks/dips each time the frequency coincides with the energy difference. Then, a different microwave frequency pulse is used to bring a coherent quantum dynamic of the qubit in the time domain [32].

The Rabi oscillations allow for the detection of relaxation time T_1. Relaxation time represents the loss of energy in the system. It is measured by sending a π pulse which fully rotates the qubit into excited state and varying the delay time before readout. Using the Ramsey interference experiment, the dephasing time T_2 can also be measured. Dephasing time shows how long the phase of a qubit will stay intact. It is measured by sending two $\pi/2$ pulses with delay time in between them. In addition, more information about decoherence time can be gathered if a π pulse is sent in between two $\pi/2$ pulses, also known as spin-echo pulse configuration [32].

The amplitude and phase of the drive can be controlled and rotations about an arbitrary x-y plane can be performed. The microwave drive resonant at qubit frequency gives rise to the Hamiltonian

$$H_{drive} = \Omega[I(t)\hat{\sigma_x} + Q(t)\hat{\sigma_y}], \tag{16}$$

where $I(t)$ and $Q(t)$ are the envelope functions of the in-phase component [33].

4.4 Spin echo

Pulses are used to dig deep into the heart of a quantum device and study the system. Quantum computers are controlled with ultra-precise pulses that stimulate the qubits and manipulate their state. Spin echo represents the spin phase information lost during the decay of the first pulse. Many of the processes which are responsible for the decay of the first pulse are reversible. The signal has not been destroyed but has become disorganized because the spins have lost their phase coherence. By applying the second pulse, certain components of the first pulse can be refocused into a spin echo [36]. The intensity of the echo is given by e^{-2t/T_2} with T_2 being the spin-spin relaxation time constant. The time between the middle of the first pulse and the peak of the spin echo is called echo time. The image of the experiment can be seen on Figure 16.

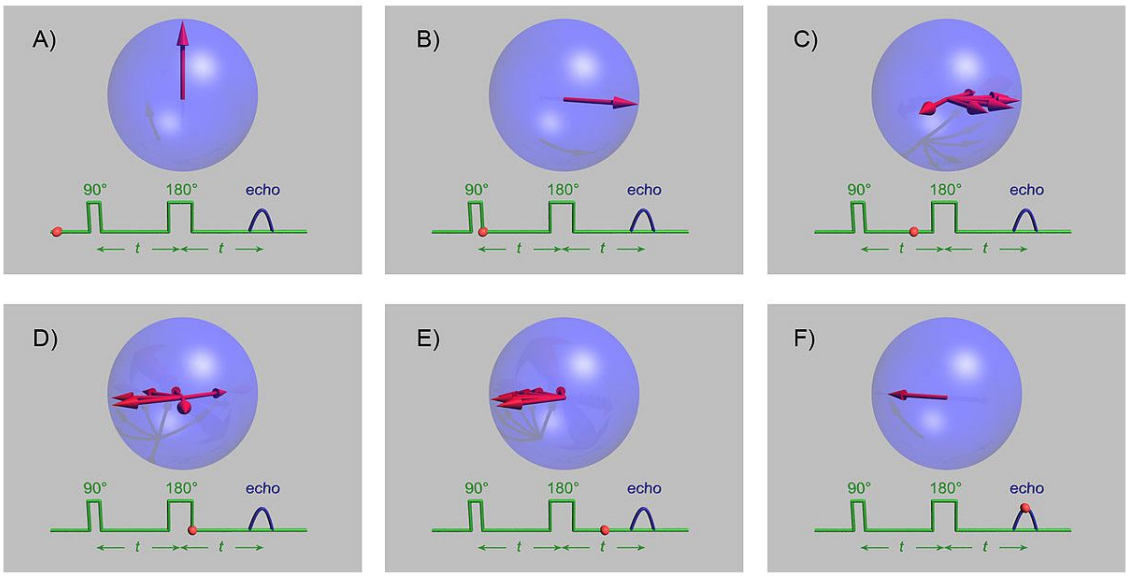

Figure 16: Red arrows represent group of spins. Some assumptions have been made like no decoherence and the environment does not provide spreading [35].

5 Data Treatment

5.1 Resonators

The quality factor (Q-factor) is a parameter which indicates the performance of a resonator circuit. It describes the damping in the circuit and indicates the energy losses with a resonant element. This links directly in to the bandwidth of a resonator with respect to its centre frequency. The higher the Q, the lower the rate of energy loss so oscillations will have low level of damping and will last longer. For circuits, energy loss caused by resistance. As the Q-factor increases, the bandwidth of the circuit filter is reduced, thus, energy is stored better in the circuit [40].

Microwave resonators are of great importance to superconducting quantum electronics. It plays a key role in quantum operations and measurement, which enables single-photon level microwave quantum optics. The improvement of the superconducting microwave resonator is the driving force in getting the qubit ready for elementary quantum computing. Hence, the coherence time of the qubits has been improved dramatically. In low-temperature microwave electronics the quality factor (inverse of the loss tangent) strongly depends on the driving microwave power. The accepted model of the power dependence of the Q-factor is the two level system model. Key breakthroughs in increasing the coherence time of the qubits were reducing the influence of charge noise by qubit design (specifically the transmon) and the strong connection between the qubit and the resonator, thus creating quantum

circuit electrodynamics (QED). Experiments suggest, that the coherence time is strongly influenced, not by the Josephson Junction, but rather by the resonator and the environmental defect. Cylindrical resonators coupled by a transmission line have proven to be very effective [37].

If multiple boundary conditions are introduced on a line, standing waves will form between the points of reflection. Transmission line resonators with high Q-factors are build from a piece of line which is either open or shortened in order to make sure the voltage reflection coefficient is very close to ± 1. Half-wave resonators have two identical boundary conditions (where both ends are shorted to ground or open) which allows for standing waves with length $\lambda_k = 2l/(k+1), k \in \mathbb{N}$. Quarter wave resonators have converse boundary conditions with one opened and one shorted, supporting $\lambda_k = 4l/(2k+1)$ [39].

The Fano quantum interference effect describes the configuration interaction between two coupled channels in a scattering problem. The scattering from an input state can form the effect either directly towards a continuum of extended states or resonantly through a discrete energy level. Equation 17 describes the Fano lineshape

$$F(\omega) = A_0 + F_0 \frac{[q + 2(\omega - \omega_0)/\Gamma]^2}{1 + [2(\omega - \omega_0)/\Gamma]^2} \tag{17}$$

where ω_0 is the frequency of the cavity mode, Γ is the resonance linewidth and A_0 and F_0 are constant factors. This equation was applied on datapoints as fit, the plot of which can be seen on Figure 17. In addition, q describes the ratio between the resonant and nonresonant transition amplitudes. Thus, there are three regimes. If $|q|$ is close to unity a strong assymetric resonance is observed. When $|q|$ is large, resonant scattering dominates and lineshape tends towards a symmetric Lorentzian. When $|q|$ is small, direct scattering dominates and lineshape takes the from of a reversed Lorentzian [41].

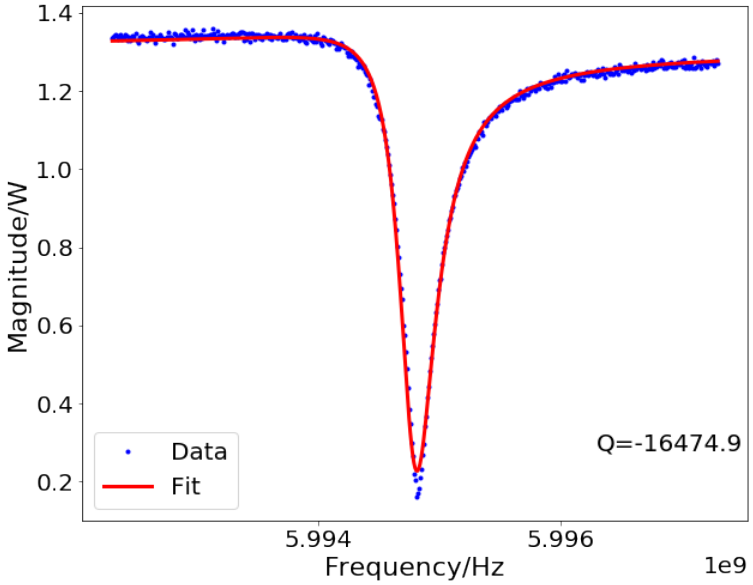

Figure 17: The transmon qubit is probed with a microwave signal and the amplitude or phase of an element of the transmitted or reflected signal is measured. The Q-factor value is approximately 16500.

5.2 Damped Rabi oscillations

This part of the experiment aims to answer the question is the system a qubit or a harmonic oscillator degree of freedom? Nothing is more fundamental in demonstrating the qubit nature of a system than Rabi oscillations. The output of a two-level system will oscillate continuously between $|0\rangle$ and $|1\rangle$ (Figure 18). In contrast, the output for a harmonic oscillator system becomes increasingly more excited as we drive power into the system with increasing drive amplitudes, never returning to the $|0\rangle$ state. When the whole system is set up, microwaves are sent to the qubit to perform manipulations on it. Frequency in the range 1-10 GHz is used. Inside the dilution refrigerator, the qubit and the microwaves can behave quantum mechanically without being disturbed by thermal noise. Microwaves trapped in the resonator can be used as a memory element to store quantum states [42]. The wavefunction then becomes,

$$|\psi(t)\rangle = \cos\left(\frac{\Omega t}{2}\right)|0\rangle + \sin\left(\frac{\Omega t}{2}\right)|1\rangle. \tag{18}$$

Where Ω is the Rabi frequency and t is time. At Ωt= 0 we get $\psi(t) = |0\rangle$, at $\Omega t = \pi$ we get $\psi(t) = |1\rangle$, at $\Omega t = 2\pi$ results in $\psi(t) = |0\rangle$, etc. Superposition can be achieved at $\Omega t = \pi/2$, then equation 18 becomes

$$|\psi\rangle = \frac{|0\rangle + |1\rangle}{\sqrt{2}}. \tag{19}$$

We can plot this relation based on probabilities, Figure 19, where probability is defined as

$$P(0) = \left| \cos\left(\frac{\Omega t}{2}\right) \right|^2 \tag{20}$$

$$P(1) = \left| \sin\left(\frac{\Omega t}{2}\right) \right|^2 \tag{21}$$

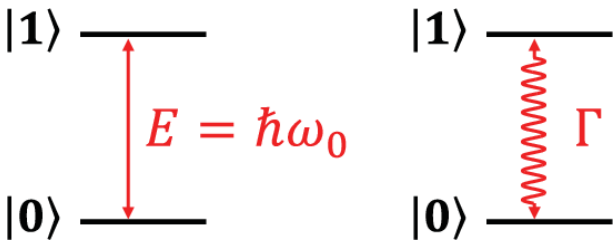

Figure 18: $|0\rangle$ is the lower energy state and $|1\rangle$ is the higher energy state, ω_0 is the transition frequency and Γ is the transition rate [43].

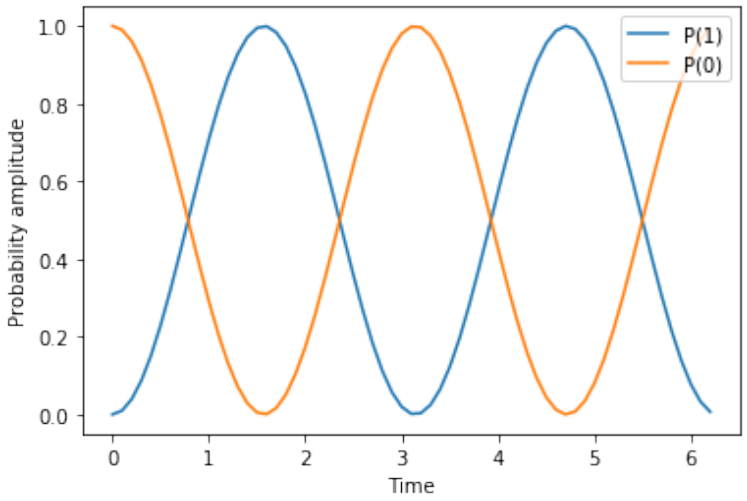

Figure 19: Probability amplitude vs time in a perfectly isolated system with no decay.

However, this describes a perfect system with no environmental influence. In reality, the probability equations 20 and 21 have an additional exponential factor $e^{-\Gamma x}$, where $\Gamma = 1/t$. It is present due to factors which cause decoherence since a system cannot be perfectly isolated from the environment. Otherwise, it would be impossible to investigate the qubit and manipulate it, hence it is not perfectly isolated during measurement and coherence is lost with time. The plot of this phenomena can be seen on Figure 20. From it, the coherence time of our transmon is measured to be 1185.26 ns.

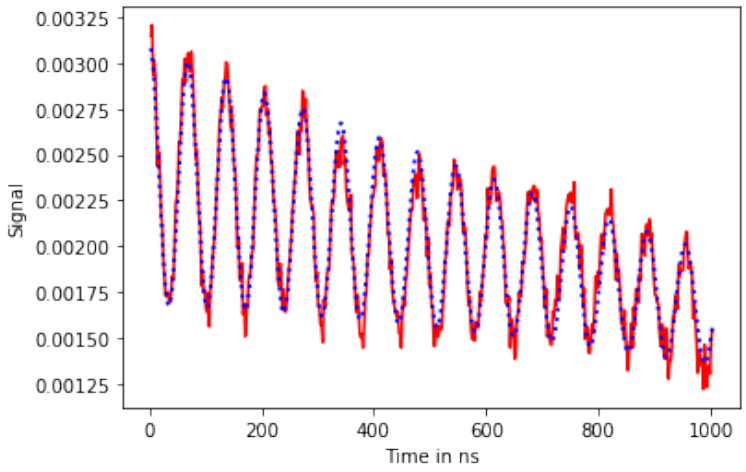

Figure 20: Rabi oscillation. The decrease is caused by the exponential factor. Decoherence represents the loss of information to the system and the collapse of the wavefunction.

5.3 Two tone spectroscopy

Once the circuit is made, the circuit parameters stay unchanged which determines the qubit energies. However, depending on the choice of qubit, its energy levels can be manipulated using a magnetic field. Magnetic field changes as we change the current through the flux bias line and the qubit frequency will change as a function of that current. Hence, fast operations can be performed to manage the chips of higher complexity where frequencies of many qubits need to be adjusted for optimum performance. Qubit energies shift in the presence of external fields [44].

Figure 21 shows the relationship between the applied magnetic field B and the frequency ω. We send a mix of two pulses (one varying pulse from VNA for qubit) and another pulse for resonator from signal generator to reach the qubit. We see that as we increase the magnetic field, the every dot of the bright lines on the Figure represents a dip of the transmission signal. Meaning, at different B we have different resonant frequencies. We get a map of signals vs different fields and pulse energies. There are two bright lines which represent the two energy levels of the transmon qubit.

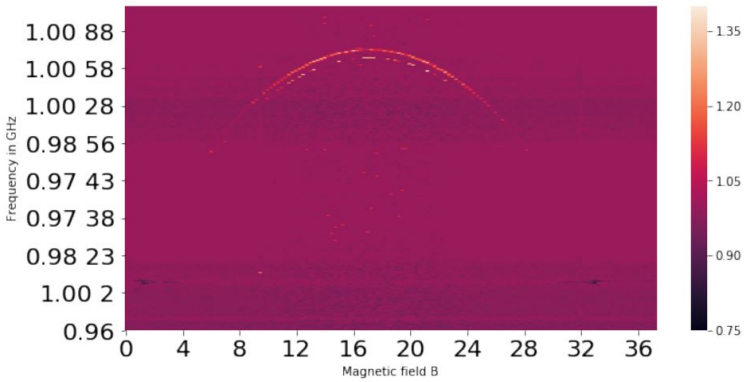

Figure 21: Energy spectra of transmon qubit

5.4 Relaxation data T_1

If we prepare the transmon qubit to be in state $|1\rangle$, we can measure the duration of time it takes for the qubit to relax in energy back to the $|0\rangle$ state. The measured data shows an exponential decay which allows us to extract the qubit's energy relaxation time, $T1$, from the time constant of the fitted decay curve.

A primary challenge in scaling circuits with superconducting qubits is not only improving their performance but also stabilizing it. It has been observed that qubit energy-relaxation times (T_1) can fluctuate unpredictably. The superconducting qubits decoherence time (which includes energy and relaxation time) is proportional to the level of dissipation which results from the coupling between the qubits and the environment. Two-level system defects are found to interact with qubits and serve as a strong energy-relaxation channel. Figure 22 shows how long it takes the qubit to transition from excited state to ground state. The time T_1 can be determined as a parameter which Python returns or graphically from the plot. Hence, it takes the qubit $T_1 \approx 1000$ ns to reach the ground state. Equation 22 was used to fit the data, with A and c being constant parameters.

$$y = Ae^{-x/T_1} + c. \tag{22}$$

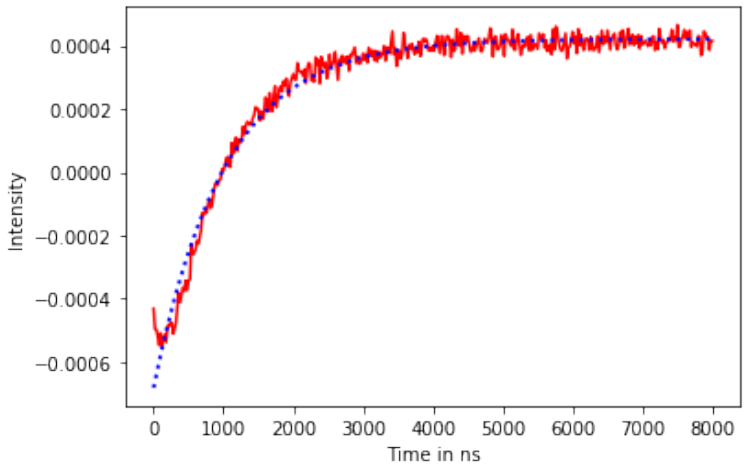

Figure 22: T1 (relaxation) data measured from spin echo experiment

6 Conclusion and Discussion

There are three basic Josephson-junction qubits: *charge qubit* (Figure 3), *flux qubit* (Figure 8) and *phase qubit* (Figure 7). Simply speaking, the charge qubit is controlled by an external voltage V_g, the flux qubit is a loop controlled by an external magnetic field Φ_{ext} and the phase qubit is Josephson junction biased by a current I_b [47].

The charge qubit is also known as a Cooper-pair box as seen on Figure 3. The heart of it is a superconducting island through which Cooper-pairs can tunnel. The island is also connected to a voltage source V_g and gate capacitance C_g. This part of the circuit determines the background charge $n_g = C_g V_g/2$ induced on the superconducting island by the electromagnetic environment. Since n_g can be controlled by an external voltage, it is possible to tune the energy levels of the system during an experiment [47].

The phase qubit consists of a large Josephson junction controlled through an applied bias current I_b. The bias current sets the tilt of the "tilted-washboard" potential for the circuit (see the lower part of Fig. 7) and is usually tuned close to the critical current I_c. The resulting eigenenergies have small anharmonicity, but the qubit can be defined as before by considering only the two lowest levels. In addition, although the phase qubit is insensitive to charge noise, there is not any symmetry point where the phase qubit is particularly well protected from noise sources [47].

The flux qubit consists of a superconducting loop interrupted by one Josephson junction. However, for this circuit to function as a qubit, there must be at least two states in the local minimum of the potential energy (see the lower part of Fig. 8). To fulfill this condition requires a large self-inductance, so the loop has to be large. This is not good when operating the circuit as a qubit, since a large loop will be more sensitive to fluctuations in external magnetic flux. A common solution to this problem is using three Josephson junctions [47].

The transmon qubit was used in this experiment. The circuit of the transmon has close resemblance to the Cooper-pair box, but it consists of an additional capacitance C_s in parallel to the Josephson junction (Figure 4). This decreases the charging energy E_C in the circuit and the resulting energy levels are insensitive to fluctuations in n_g. This protection from charge noise decreases the anharmonicity of the circuit [47]. Data of the transmon qubit was analysed. The coherence time was measured to be 1185.26 ns. Two energy levels were examined using two tone spectroscopy. The relaxation time T_1 was found to be 1000 ns.

References

[1] *Qubit*, Wikipedia, Feb 24 2021

[2] *Superconducting quantum bits*, Physics World, Dec 01 2004

[3] *How to make artificial atoms out of electrical circuits*, Christian Dickel, QuTech, Mar 14 2017

[4] *The Quantum Harmonic Oscillator*, BCcampus Open Publishing

[5] *Quantum decoherence*, Wikipedia, Feb 3 2021

[6] *Quantum noise*Wikipedia

[7] *Spectral Analysis and Identification of Noises in Quantum Systems*, Franco Nori, Research Gate Nov 2012

[8] Y. Nakamura. "Coherent control of macroscopic quantum states in a single-Cooper-pair box". In: *Letters to Nature* (29 April 1999)

[9] N. Yanofsky and M. Mannucci. "Quantum computing for computer scientists". In: *Cambridge Press* (2008)

[10] *Josephson Junction* HyperPhysics Concepts, Ohanian, Hans, Physics, 2E Expanded, WW Norton 1989

[11] *How to make artificial atoms out of electrical circuits–Part II*, Christian Dickel, QuTech, Aug 12 2017

[12] *Schematic diagram of ac Josephson junction*, Md. Rafiqul Islam, Research Gate

[13] Gustav Andersson. "Circuit quantum electrodynamics with a transmon qubit in a 3D cavity" . *Technical University of Munich.* (March 2015)

[14] *Transmon*, Wikipedia, Dec 1 2020.

[15] John M. Martinis. "Superconducting Phase Qubits". 2008

[16] Alexandre Zagoskin. Superconducting qubits. *University of British Columbia.* (May 1 2008)

[17] *Silicon Wafer Processing*, Wafer World, Apr 09 2018

[18] *History of Silicon Wafers*, Vintage Computer Chip Collectibles

[19] *Photolithography: Exposure and resist coating*, Semiconductor Technology

[20] *Photolithography*, TechTarget, Aug 2013

[21] *PicoMaster 100 Direct Laser Writer*, 4PICO

[22] *Electron Beam Lithography*, Nanolithography Techniques, July 18 2018

[23] *Plassys Electron Beam Evaporation System*, University of Pittsburgh

[24] *What is physical vapour deposition (PVD)?* , TWI Ltd

[25] *Thin film deposition*, Florence Billon, Laboratoire Interfaces et Systèmes Electrochimiques

[26] *Superconductivity*, CERN

[27] *Dilution Refrigerators*, Dr. John Weisend, Cryogen Society of America, July 5 2012

[28] "Essential Hardware Components of a Quantum Computer". National Academies of Sciences, Engineering, and Medicine. 2019. Quantum Computing: Progress and Prospects. Washington, DC: The National Academies Press. doi: 10.17226/25196.

[29] r/Physics

[30] *Quantum logic gate*, Wikipedia, Feb 22 2021

[31] *Rabi frequency*, Wikipedia, Sep 17 2020

[32] Y. Nakamura, I. Chiorescu. "Coherent Quantum Dynamics of a Superconducting Flux Qubit". *Delft University of Technology*. (20 May 2003)

[33] Morten Kjaergaard. "Superconducting Qubits: Current State of Play". In: *Annual Reviews*. (17 December 2019)

[34] *What is NMR?*, NMR Lab

[35] *Spin echo*, Wikipedia, 20 October 2020

[36] L. Hahn. "Spin Echo". In: *Physical Review*. (November 15 1950)

[37] Yonuk Chong. "A brief review on recent developments of superconducting microwave resonators for quantum device application". *Korea Research Institute of Standards and Science*. (13 October 2014)

[38] Ren-Shou Huang. "Qubit-Resonator system as an application to quantum computation". *Department of Physics, Indiana University*. (May 2004)

[39] Prof. Dr. Alexey V. Ustinov. "Experiments on Superconducting Qubits Coupled to Resonators". (1 February 2013)

[40] *Quality Factor*, Electronics Notes

[41] M. Galli. "Light scattering and Fano resonances in high-Q photonic crystal nanocavities". Appl. Phys. Lett. 94, 071101 (2009);

[42] *Superconducting Quantum Circuits*, Microscoping quantum machines

[43] C. Degen. *Quantum sensing*. Semantic Scholar. Published in 2016

[44] *How to make artificial atoms out of electrical circuits–Part II*, Christian Dickel, QuTech, Aug 12 2017

[45] Philipp Treutlein. *Photon Qubit is Made of Two Colors*. APS Physics. Department of Physics, University of Basel. November 23, 2016

[46] A. Wallraff. "Sideband Transitions and Two-Tone Spectroscopy of a Superconducting Qubit Strongly Coupled to an On-Chip Cavity". In: *Physical Review Letters*. PRL 99, 050501 (2007)

[47] Kockum A.F., Nori F. (2019) Quantum Bits with Josephson Junctions. In: Tafuri F. (eds) Fundamentals and Frontiers of the Josephson Effect. Springer Series in Materials Science, vol 286. Springer, Cham. https://doi.org/10.1007/978-3-030-20726-7_17